crystals

MDPI

Article

Synthesis, Crystal Structure and Photoluminescent Properties of Novel 9-Cyano-Pyrrolo[1,2-*a*][1,10]Phenanthrolines

Mihaela Cristea [1], Mihai Răducă [1,2,*], Sergiu Shova [3], Constantin Drăghici [1], Vlad A. Neacșu [2,4], Maria Maganu [1], Loredana Albotă (Barbu) [1], Denisa Dumitrescu [5] and Florea Dumitrascu [1,*]

[1] "C. D. Nenițescu" Institute of Organic and Supramolecular Chemistry, Romanian Academy, 202 B Splaiul Independenței, 060023 Bucharest, Romania; mihcris2012@yahoo.ro (M.C.); cst_drag@yahoo.com (C.D.); mmaganu@yahoo.com (M.M.); lobarbu68@yahoo.com (L.A.)
[2] Inorganic Chemistry Department, Faculty of Chemistry, University of Bucharest, Regina Elisabeta Blvd., 4-12, 030018 Bucharest, Romania; vlad.neacsu2009@gmail.com
[3] Department of Inorganic Polymers, Petru Poni Institute of Macromolecular Chemistry, Aleea Grigore Ghica Vodă nr. 41A, 700487 Iași, Romania; shova@icmpp.ro
[4] Department of Chemistry, City University of Hong Kong, 83 Tat Chee Avenue, Kowloon Tong, Hong Kong 999077, China
[5] Faculty of Pharmacy, Ovidius University Constanta, Campus Corp C, Str. Cpt. Av. Al. Serbanescu, 900470 Constanta, Romania; denisa.dumitrescu2014@gmail.com
* Correspondence: fiidemn@gmail.com (M.R.); fdumitra@yahoo.com (F.D.)

Abstract: Novel 9-cyano-pyrrolo[1,2-*a*][1,10]phenanthrolines **6a–d** were obtained by an efficient one-pot regioselective reaction between 1,10-phenanthrolinium bromides **2a–d** and acrylonitrile as a dipolarophile, in the presence of triethylamine and tetrakis-pyridino-cobalt(II) dichromate (TPCD) as oxidizing agents. The optical properties of the compounds were investigated through UV–Vis spectrophotometry and steady-state photoluminescence measurements, while their structures were elucidated by single-crystal X-ray diffraction. The structural characterization revealed that the molecular structures of the four compounds were stabilized by hydrogen bonds and π–π interactions.

Keywords: pyrrolo[1,2-*a*][1,10]phenanthrolines; 1,10-phenanthrolinium *N*-ylide; 1,3-dipolar cycloaddition; helical chirality; X-ray diffraction

Citation: Cristea, M.; Răducă, M.; Shova, S.; Drăghici, C.; Neacșu, V.A.; Maganu, M.; Albotă, L.; Dumitrescu, D.; Dumitrascu, F. Synthesis, Crystal Structure and Photoluminescent Properties of Novel 9-Cyano-Pyrrolo[1,2-*a*][1,10]Phenanthrolines. *Crystals* **2024**, *14*, 67. https://doi.org/10.3390/cryst14010067

Academic Editors: Ana M. Garcia-Deibe and Aidar T. Gubaidullin

Received: 11 December 2023
Revised: 29 December 2023
Accepted: 4 January 2024
Published: 7 January 2024

1. Introduction

Pyrrolo[1,2-*a*][1,10]phenanthroline **1** is an *N*-bridgehead aromatic heterocycle, formally obtained by the condensation of 1,10-phenanthroline and pyrrole. The numbering of the atoms from the pyrrolo[1,2-*a*][1,10]phenanthroline skeleton is presented in Figure 1.

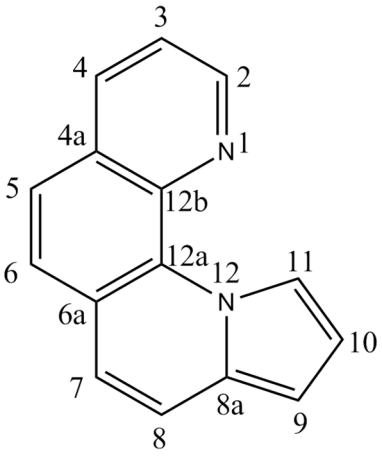

Figure 1. Structure of pyrrolo[1,2-*a*][1,10]phenanthroline **1**. The numbering scheme is presented in agreement with rules for IUPAC.

The number of methods that allow the synthesis of pyrrolo[1,2-*a*][1,10]phenanthroline derivatives is still limited, and all reported methods use 1,10-phenantroline as a key precursor.

The first pyrrolo[1,2-*a*][1,10]phenanthroline derivatives were synthesized by Dumitrascu et al. in 2001 through a [3+2] cycloaddition reaction [1]. While novel methods for the synthesis of these compounds have been described [2–9], the main approach continues to be the 1,3-dipolar cycloaddition reaction [1,4,10–17].

The 1,10-phenanthroline derivatives and fused pyrrolo-1,10-phenanthroline type derivatives display interesting properties, not only from a chemical point of view (synthesis, reactivity, stereochemistry, aromaticity [18], basicity [19] and chelating capacity [20]), but also in terms of their biological [10,21–26], electrical [27–29] and optical properties [30]. Some pyrrolo[1,2-*a*][1,10]phenanthroline derivatives have potential applications in materials science as organic light-emitting diodes [30–32], being promising candidates for solid-state device technology.

Previous NMR studies revealed the non-equivalence of the diastereotopic methylene and methyl hydrogens in the prochiral groups (ethyl, isopropyl) of pyrrolo[1,2-*a*][1,10]phenanthroline esters [1,4,15], which was further confirmed by X-ray diffraction experiments [5,33,34]. Furthermore, NMR data and single-crystal X-ray diffraction unveiled the existence of helical chirality in the pyrrolo[1,2-*a*][1,10]phenanthroline skeleton, similar to that of helicene-type compounds [1,5,35].

The reaction between phenanthrolinium *N*-ylides and dipolarophilic alkenes is less studied [4,14]. Recently, the reaction of 1,10-phenanthrolinium *N*-ylides with acrylonitrile leading to dihydro-pyrrolo[1,2-*a*][1,10]phenanthrolines was reported [17].

Herein, we describe the synthesis and single-crystal X-ray diffraction of new 9-cyano-pyrrolo[1,2-*a*][1,10]phenanthrolines **6a**–**d**, obtained by the 1,3-dipolar cycloaddition of 1,10-phenanthrolinium *N*-ylides and acrylonitrile, in the presence of triethylamine and tetrakis-pyridino-cobalt(II) dichromate (TPCD) as oxidant reagent. Their general structures are represented in Figure 2.

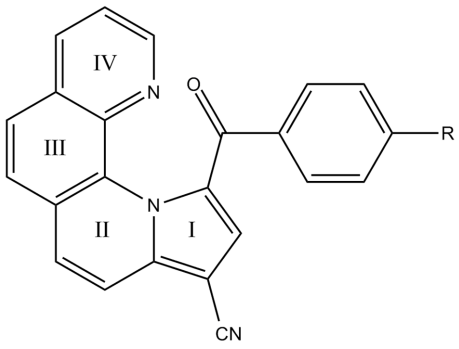

6a-d

6a: R = H; **6b:** R = -C_6H_{11}; **6c:** R = OMe; **6d:** R = CN

Figure 2. General structure of 9-cyano-pyrrolo[1,2-*a*][1,10]phenanthrolines **6a**–**d**. The four condensed cycles are numbered with Roman numerals from I to IV.

2. Materials and Methods

2.1. Chemicals and Instrumentation

Melting points were determined on a Boëtius hot plate apparatus and are uncorrected. NMR spectra were recorded on a Varian Gemini 300 BB instrument, operating at 300 MHz for ^{1}H and 75 MHz for ^{13}C. Supplementary evidence was given by HETCOR and COSY experiments. All chemical shifts (δ values) are given in parts per million (ppm); all homo- and heterocoupling patterns (^{n}J values) are given in hertz (Hz). No TMS was added, and chemical shifts were measured against the solvent peak. The electronic absorption spectra were measured using a UV–Vis spectrometer, the Carry 100 Bio (JASCO, Tokyo, Japan). The UV–Vis absorption and emission spectra of the investigated compounds were

recorded in dilute solution (2×10^{-5} mol/L), using acetonitrile of HPLC purity (ACN, Scharlau, Barcelona, Spain). All experiments were performed at 25 °C. All measurements were performed in single-beam mode in the 200–800 nm range, using a 1 cm pathlength quartz cuvette. The baseline corrections were performed with air and the spectrum of the blank sample (accounting for the contribution of the cuvette and the solvent) was subtracted from each spectrum. The molar extinction coefficients were determined from the absorption spectra of the solutions of each compound with known concentrations using the Lambert–Beer law. The steady-state photoluminescence spectra were measured using an FP-6500 spectrofluorometer (JASCO, Japan) with a xenon arc lamp as an excitation source. All spectra were corrected for background and the excitation spectra were additionally corrected for lamp power. Unless stated otherwise, the excitation and emission slits for all steady-state photoluminescence experiments were 5 nm. The IR spectra were recorded using an FT-IR Bruker Vertex 70 equipped with a reflectance device (ATR) with a diamond crystal and a device with PM IRRAS and VCD extensions, equipped with a cell with a CaF_2 window. IR spectra were processed with the OPUS 5.5 (Bruker) software. The elemental analysis was carried out on a Perkin Elmer CHN 240 B apparatus. The compounds' nomenclature was taken from the Cambridge Soft package's structure-to-name algorithm included with Chem Bio Draw Ultra 11.0.

The X-ray diffraction measurements for **6b** and **6c** were carried out with a Rigaku Oxford Diffraction XCALIBUR E CCD diffractometer (Rigaku, Tokyo, Japan) equipped with graphite-monochromated Mo-Kα radiation (λ = 0.71073 Å), and those for **6a** and **6d** were carried out with a Rigaku XtaLAB Synergy-D diffractometer operating with a Cu-Kα (λ = 1.54184 Å) micro-focus sealed X-ray tube. The structures were solved by Intrinsic Phasing using the Olex2 software version 1.5 [36] with the SHELXT structure solution program [37] and refined using full-matrix least-squares on F2 with SHELXL-2015 [38] using an anisotropic model for non-hydrogen atoms. A summary of the crystallographic data and the structure refinement is given in Table 1. Deposition numbers for **6a** (2296260), **6b** (2296259), **6c** (2296258) and **6d** (2296261) contain the supplementary crystallographic data for this paper. These data are provided free of charge by the joint Cambridge Crystallographic Data Centre and Fachinformationszentrum Karlsruhe Access Structures service www.ccdc.cam.ac.uk/structures (accessed on 10 December 2023).

Table 1. Crystallographic data and structure refinement for compounds **6a–d**.

Compound	**6a**	**6d**	**6c**	**6b**
Chemical formula	$C_{23}H_{13}N_3O$	$C_{24}H_{12}N_4O$	$C_{24}H_{15}N_3O_2$	$C_{29}H_{23}N_3O$
M (g mol^{-1})	347.36	372.38	377.39	429.50
Temperature (K)	100	100	293	293
Wavelength (Å)	1.54184	1.54184	0.71073	0.71073
Crystal system	*Monoclinic*	*Monoclinic*	*Monoclinic*	*Monoclinic*
Space group	$P2_1/c$	$C2/c$	$I2/a$	$P2_1/c$
a (Å)	12.1607(3)	19.2428(2)	12.6943(9)	12.9773(6)
b (Å)	11.3417(3)	7.89850(9)	11.1317(5)	9.9248(3)
c (Å)	12.4199(3)	23.3102(2)	26.3923(15)	17.4660(7)
α (°)	90	90	90	90
β (°)	102.809(2)	90.7499(10)	98.355(6)	101.806(4)
γ (°)	90	90	90	90
V (Å^3)	1670.36(7)	3542.60(7)	3689.9(4)	2201.98(15)
Z	4	8	8	4
D_c (g cm^{-3})	1.381	1.396	1.359	1.296
μ(mm^{-1})	0.694	0.714	0.089	0.080
F(000)	720	1536	1568	904
2Θ range for data collection (°)	7.456 to 153.988	7.586 to 153.9	4.89 to 50.7	4.746 to 50.698
Index ranges	$-15 \le h \le 10$, $-13 \le k \le 12$, $-15 \le l \le 15$	$-23 \le h \le 23$, $-8 \le k \le 9$, $-28 \le l \le 25$	$-15 \le h \le 14$, $-12 \le k \le 13$, $-29 \le l \le 31$	$-15 \le h \le 15$, $-11 \le k \le 10$, $-21 \le l \le 21$
Reflections collected	10,892	13,114	11,224	13,519
Independent reflections	3218 [R_{int} = 0.0352, R_{sigma} = 0.0376]	3424 [R_{int} = 0.0179, R_{sigma} = 0.0151]	3381 [R_{int} = 0.0350, R_{sigma} = 0.0499]	4029 [R_{int} = 0.0381, R_{sigma} = 0.0516]
Data/restraints/parameters	3218/0/244	3424/0/263	3381/0/264	4029/0/299
GOF	1.039	1.032	1.024	1.049
Final R_1, wR_2 [I > 2σ(I)]	0.0378, 0.0970	0.0330, 0.0900	0.0512, 0.0948	0.0514, 0.0932
R_1, wR_2 (all data)	0.0463, 0.1034	0.0350, 0.0918	0.0899, 0.1077	0.0861, 0.1063
$\Delta\rho_{min}/\Delta\rho_{max}$ (e Å^{-3})	0.20, −0.21	0.23, −0.19	0.13, −0.15	0.17, −0.14

All commercially available products were used without further purification, unless otherwise specified. All chemicals for the syntheses were purchased from commercial sources.

2.2. Synthesis and Characterization

General procedure for the one-pot synthesis of 9-cyano-pyrrolo[1,2-a][1,10]phenanthrolines **6a–d**.

A solution of 1,10-phenanthrolinium bromide derivative **1a–d** (5 mmol), acrylonitrile (15 mmol), triethylamine (6 mmol) and TPCD (5 mmol) in DMF (30 mL) was stirred at 80–90 °C for 6 h. It was then cooled down to room temperature and a 5% (*v*/*v*) aqueous HCl solution (100 mL) was added. The precipitate was filtered and purified by crystallization from nitromethane. The 9-cyano-pyrrolo[1,2-*a*][1,10]phenanthrolines **6a–d** were obtained with 50–60% yields.

11-Benzoylpyrrolo[1,2-a][1,10]phenanthroline-9-carbonitrile (**6a**)

Yellow crystals, platelets, obtained from nitromethane, m.p. 247–250 °C; yield 60%. Elemental analysis: Found for $C_{23}H_{13}N_3O$: C 79.77; H 4.04; N 12.37. Calculated: C 79.53; H 3.77; N 12.10. UV–VIS (MeCN), λ (log ε): 225 (4.72), 242 (4.62), 275 (4.49), 310 sh (4.21), 374 (3.79). FT-IR (cm^{-1}): 3111 m, 3061 m, 2313 w, 2203 vs, 1703 w, 1634 vs, 1587 s, 1531 s, 1486 s, 1440 s, 1352 s, 1282 s, 1134 s, 1012 s, 975 vs, 694 vs, 669 vs. ^{1}H-NMR ($CDCl_3$; δ, ppm; *J*, Hz): 7.35 (s, 1H, H-10); 7.38 (dd, 8.0, 4.5, H-3); 7.54–7.60 (m, 2H, H-3′, H-5′); 7.64–7.70 (m, 1H, H-4′); 7.72 (d, 1H, 9.1, H-7); 7.83 (d, 1H, 8.6, H-5); 7.88 (d, 1H, 8.6, H-6); 7.91 (d, 1H, 9.1, H-8); 8.18–8.30 (m, 4H, H-2, H-4, H-2′, H-6′). ^{13}C-NMR ($CDCl_3$; δ, ppm): 85.2 (C-9); 116.0 (CN); 117.9 (C-8); 121.4 (C-10); 122.9 (C-3); 125.6, 128.0, 129.7, 133.4, 137.7, 140.7 (C-4a, C-6a, C-8a, C-11, C-12a, C-12b); 125.7 (C-5); 126.1 (C-6); 126.6 (C-7); 128.6 (C-3′, C-5′); 130.3 (C-2′, C-6′); 132.9 (C-4′); 136.1 (C-4); 137.1 (C-1′); 146.4 (C-2); 184.4 (CO).

11-(4-Cyclohexylbenzoyl)pyrrolo[1,2-a][1,10]phenanthroline-9-carbonitrile (**6b**)

Yellow crystals, platelets, obtained from nitromethane, m.p. 265–267 °C; yield 57%. Elemental analysis: Found for $C_{29}H_{23}N_3O$:C, 81.31; H, 5.67; N, 10.17. Calculated C, 81.09; H, 5.40; N, 9.78. UV–VIS (MeCN), λ (log ε): 224 (4.68), 244 (4.59), 272 (4.57), 310 sh (4.23), 371 (3.78). FT-IR (cm^{-1}):3105 s, 3035 m, 2927 vs, 2849 s, 2205 vs, 1696 vs, 1630 vs, 1596 vs, 1487 s, 1442 s, 1399 s, 1350 s, 1289 s, 1203 s, 1164 s, 1132 s, 873 s, 833 vs, 688 s. ^{1}H-NMR ($CDCl_3$; δ, ppm; *J*,Hz): 1.25–2.00 (m, 10H, cyclohexyl); 2.62–2.70 (m, 1H, cyclohexyl), 7.35–7.41 (m, 4H, H-3, H-10, H-3′, H-5′); 7.69 (d, 1H, 9.1, H-7); 7.80–7.91 (m, 1H, 8.6, H-5, H-6, H-8); 8.12–8.20 (m, 4H, H-2, H-4, H-2′, H-6′). ^{13}C-NMR ($CDCl_3$; δ, ppm): 26.2, 26.9, 34.4, 44.4 (6C, cyclohexyl); 85.1 (C-9); 116.1 (CN); 117.9 (C-8); 121.5 (C-10); 122.8 (C-3); 125.5, 127.9, 129.7, 133.7, 137.8, 140.6 (C-11, C-8a, C-6a, C-4a, C-13b, C-13a); 125.6 (C-5); 126.0 (C-6); 126.6 (C-7); 127.0 (C-3′, C-5′); 130.5 (C-2′, C-6′); 134.8 (C-1′); 136.0 (C-4); 140.6 (C-4′), 146.5 (C-2); 184.4 (CO).

11-(4-Methoxybenzoyl)pyrrolo[1,2-a][1,10]phenanthroline-9-carbonitrile (**6c**)

Yellow crystals, platelets, obtained from nitromethane, m.p. 245–247 °C; yield 52%. Elemental analysis: Found for $C_{24}H_{15}N_3O_2$: C, 76.69; H, 4.33; N, 11.41. Calculated: C, 76.38; H, 4.01; N, 11.13. UV–VIS (MeCN), λ (log ε): 224 (4.71), 242sh (4.54), 275 (4.59), 310 sh (4.34), 371 (3.89). FT-IR (cm^{-1}):3046 w, 2941 w, 2836 w, 2204 vs,1693 vs, 1632 vs, 1592 vs, 1489 s, 1396 m, 1312 s, 1248 vs, 1151 vs, 905 s, 839 vs, 689 m. ^{1}H-NMR ($CDCl_3$; δ, ppm; *J*,Hz): 3.95 (m, 3H, OMe); 7.05–7.08 (m, 2H, H-3′, H-5′); 7.34 (s, 1H, H-10); 7.38 (dd, 8.0, 4.5, H-3); 7.72 (d, 1H, 9.1, H-7); 7.83 (d, 1H, 8.6, H-5); 7.88 (d, 1H, 8.6, H-6); 7.91 (d, 1H, 9.1, H-8); 8.19–8.23 (m, 4H, H-2, H-4, H-2′, H-6′). ^{13}C-NMR ($CDCl_3$; δ, ppm): 55.7 (MeO); 85.1 (C-9); 113.8 (C-3′, C-5′); 116.1 (CN); 118.0 (C-8); 121.2 (C-10); 122.9 (C-3); 125.6, 127.9, 129.8, 133.5, 137.9, 140.6 (C-4a, C-6a, C-8a, C-11, C-12a, C-12b); 125.6 (C-5); 126.0 (C-6); 126.6 (C-7); 129.9 (C-1′); 132.4 (C-2′, C-6′); 163.5 (C-4′); 136.0 (C-4); 146.4 (C-2); 184.1 (CO).

11-(4-Cyanobenzoyl)pyrrolo[1,2-a][1,10]phenanthroline-9-carbonitrile (**6d**)

Yellow crystals obtained from nitromethane, m.p. 287–290 °C; yield 50%. Elemental analysis: Found for $C_{24}H_{14}N_4O$: C, 77.35; H, 4.09; N, 15.27. Calculated: C, 76.99; H, 3.77; N, 14.96. UV–VIS (MeCN), λ (log ε): 226 (4.70), 247 (4.71), 286 (4.44), 310 sh (4.23), 388 (3.79). FT-IR (cm^{-1}):3083 w, 3048 w, 2929 w, 2856 w,2208 vs, 1645 vs, 1565 s, 1535 s, 1487 s, 1443 s, 1355 s, 1285 s, 1196 s, 1138 s, 1016 s, 865 vs. ^{1}H-NMR ($CDCl_3$; δ, ppm; *J*,Hz): 3.95 (m, 3H,

OMe); 7.05–7.08 (m, 2H, H-3′, H-5′); 7.34 (s, 1H, H-10); 7.38 (dd, 8.0, 4.5, H-3); 7.72 (d, 1H, 9.1, H-7); 7.83 (d, 1H, 8.6, H-5); 7.88 (d, 1H, 8.6, H-6); 7.91 (d, 1H, 9.1, H-8); 8.19–8.23 (m, 4H, H-2, H-4, H-2′, H-6′). ^{13}C-NMR ($CDCl_3$; δ, ppm): 85.6 (C-9); 115.6, 116.1 (2CN); 118.0 (C-8); 117.2 (C-4′); 121.4 (C-10); 123.1 (C-3); 125.7, 128.1, 129.4, 132.2, 137.4, 140.8 (C-4a, C-6a, C-8a, C-11, C-12a, C-12b); 125.7 (C-5); 126.0 (C-6); 126.5 (C-7); 128.1 (C-2′, C-6′); 132.2 (C-1′); 132.5 (C-3′, C-5′); 136.4 (C-4); 146.2 (C-2); 182.3 (CO).

3. Results and Discussion

3.1. Syntheses

The 9-cyano-pyrrolo[1,2-*a*][1,10]phenanthrolines **6a–d** were obtained from 1-(4-phenylphenacyl)-1,10-phenanthrolinium bromides **2a–d**, acrylonitrile and triethylamine in DMF at 80–90 °C, using tetrakis-pyridine cobalt (II) dichromate ($Py_4Co(HCrO_4)_2$, TPCD) as an oxidant (Scheme 1). The bromide precursors **2a–d** were easily prepared by the N-alkylation of 1,10-phenanthroline hydrate with 2′-bromo-4′-phenylacetophenones in acetone under reflux, as previously reported [4].

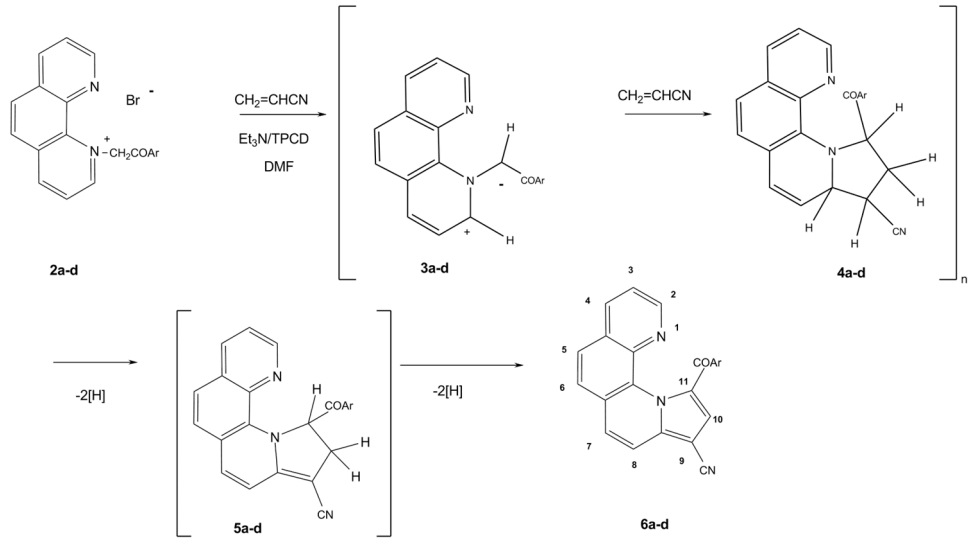

Scheme 1. The reaction scheme of 9-cyano-pyrrolo[1,2-*a*][1,10]phenanthrolines **6a–d**. **6a:** Ar = C_6H_5; **6b:** Ar = 4−$C_6H_{11}C_6H_4$; **6c:** Ar = 4−$MeOC_6H_4$; **6d:** 4−CNC_6H_4. The numbering scheme of **6a–d** is presented in agreement with rules for IUPAC.

The synthesis of pyrrolo[1,2-*a*][1,10]phenanthroline derivatives from activated alkenes and 1,10-phenanthrolinium N-ylides first involves the formation of tetrahydro-pyrrolo[1,2-*a*][1,10]phenanthrolines, which are relatively stable in the reaction conditions.

The reaction mechanism (Scheme 1) consists, in the first step, of the deprotonation of cycloimmonium salts **2a–d** in the presence of triethylamine, yielding the unstable 1,10-phenanthrolinium *N*-ylides **3a–d**. The aromatization of tetrahydro-pyrrolo[1,2-*a*][1,10]phenanthrolines **4a–d** obtained by the [3+2] dipolar cycloaddition between the unstable 1,10-phenanthrolinium *N*-ylides **3a–d** and acrylonitrile to pyrrolo[1,2-*a*][1,10]phenanthrolines **6a–d** was performed using TPCD as oxidizing agent [39].

3.2. X-ray Crystallography

The crystal structures of compounds **6a–d** show similar features. Compound **6a** (Figure 3) crystalizes in a monoclinic crystal system, in the $P2_1/c$ space group (Table 1). The dihedral angle ∠(C3-C4-C5),(C23-C18-C19), between the pyrrolic ring and the benzene ring, is 66.3°. The phenanthroline units are stacked with π–π stacking centroid–centroid distances around 3.67 Å (Figure 4a). The ketonic oxygen O1 forms two hydrogen bonds with the neighboring molecule. The O1···H(-C8*) distance for the first intermolecular hydrogen interaction is 2.309 Å (O1···C8* = 3.193 Å) and the corresponding O1···H-C8* angle is

154.4°, while, for the second one, it is O1···H(-C10*) = 2.681 Å (O1···C10* = 3.473 Å) and the O1···H-C10* angle is 141.3° (Figure 4b) (symmetry operation * = 1−x, −1/2+y, 1/2−z).

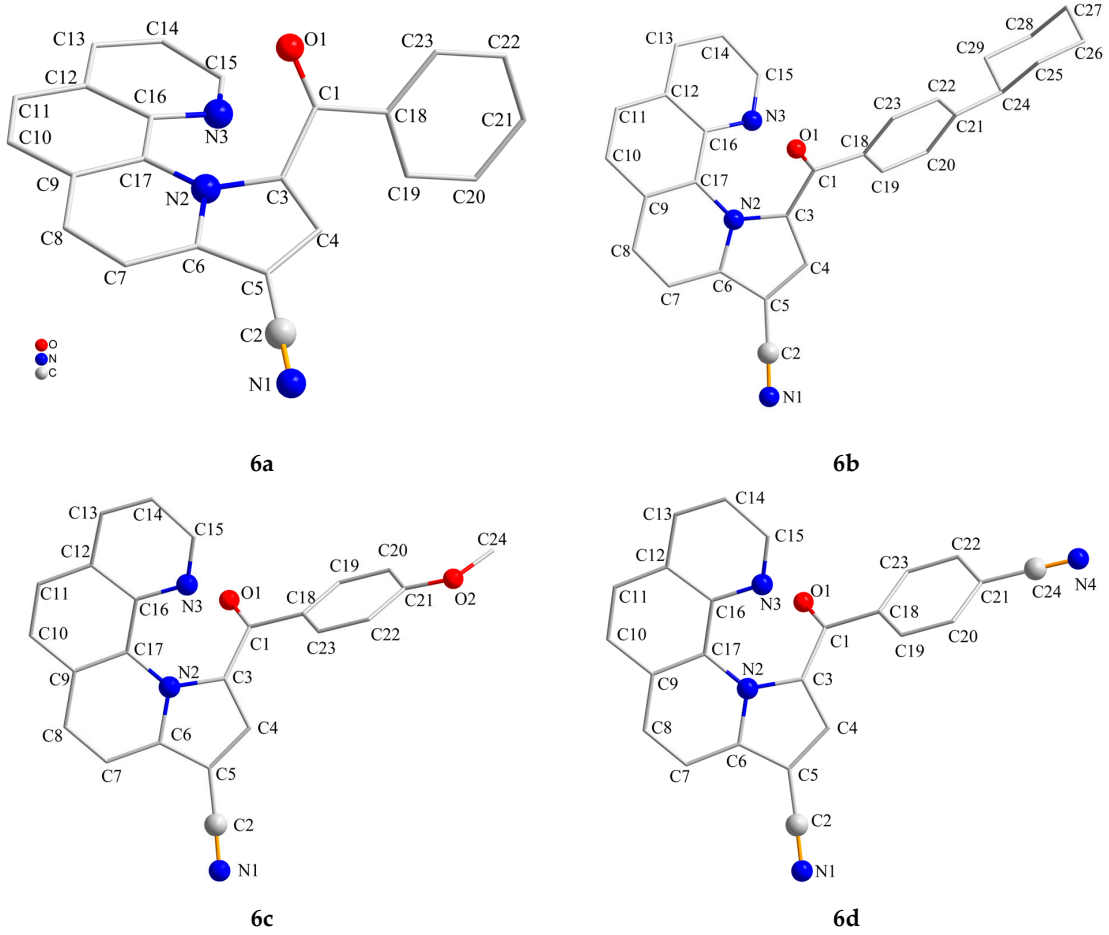

Figure 3. Perspective views of the crystal structures of compounds **6a–d** and the numbering scheme for each atom. Hydrogen atoms have been neglected in the representation.

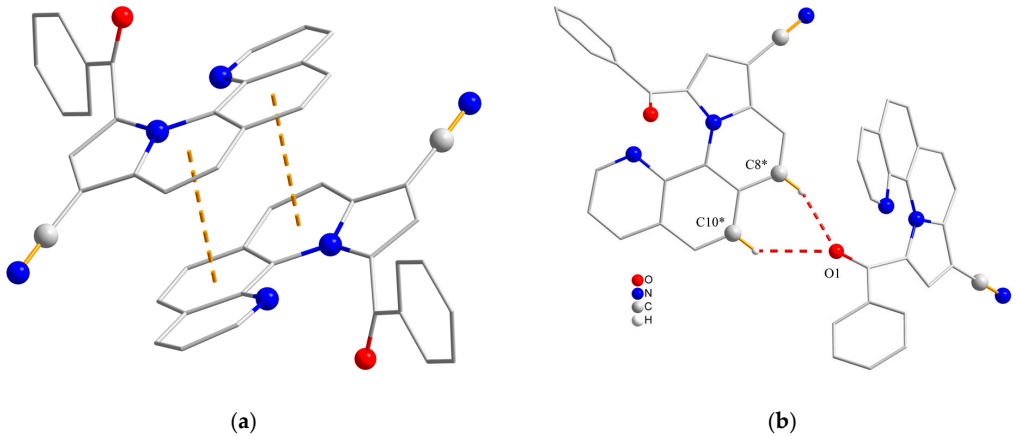

Figure 4. Perspective view of **6a** showing (**a**) the π–π stacking interactions between two neighboring phenanthroline units and (**b**) the hydrogen bonds formed by the oxygen from the ketone unit (symmetry operation * = 1−x, −1/2+y, 1/2−z). Hydrogen atoms have been omitted, except those involved in hydrogen bonds.

Compound **6b** (Figure 3) crystalizes in a monoclinic crystal system, in the $P2_1/c$ space group (see Table 1). The dihedral angle ∠(C3-C4-C5),(C23-C18-C19), between the pyrrolic

ring and the benzene ring, is 55.9°. The phenanthroline units are stacked with π–π stacking centroid–centroid distances around 3.94 Å (Figure 5a). The ketonic oxygen O1 forms two hydrogen bonds with two neighboring molecules. The O1···H(-C4d) distance for the first intermolecular hydrogen interaction is 2.411 Å (O1···C4d = 3.344 Å) and the corresponding O1···H-C4d angle is 171.7°, while, for the second one, it is O1···H(-C11e) = 2.469 Å (O1···C11e = 3.288 Å) and the O1···H-C11e angle is 146.8° (Figure 5b) (symmetry operations d = 1−x, −1/2+y, 3/2−z; e = 1−x, −y,1−z).

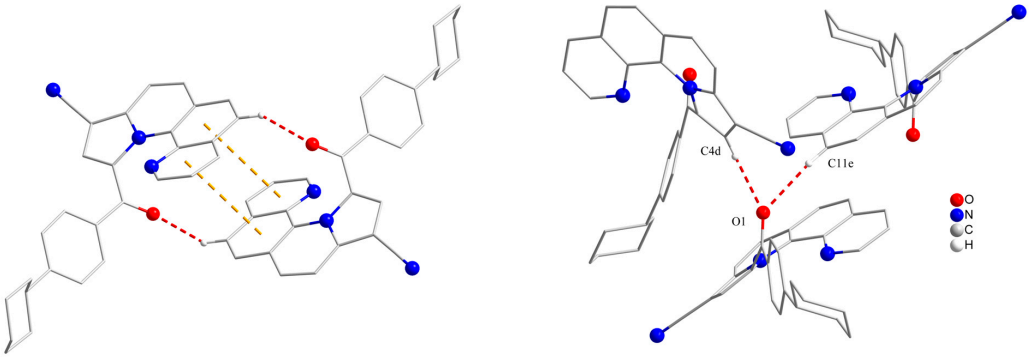

(**a**) (**b**)

Figure 5. Perspective view of **6b** showing (**a**) the π–π stacking interactions between two neighboring phenanthroline units and (**b**) the hydrogen bond formed by the oxygen from the ketone unit (symmetry operations d = 1−x, −1/2+y, 3/2−z; e = 1−x, −y,1−z). Hydrogen atoms have been omitted, except those involved in hydrogen bonds.

Compound **6c** (Figure 3) crystalizes in a monoclinic crystal system, in the *I*2/*a* space group (Table 1). The dihedral angle ∠(C3-C4-C5),(C23-C18-C19), between the pyrrolic ring and the benzene ring, is 70.1°. CH–π interactions are established between neighboring phenanthroline units with CH–centroid distances around 3.00 Å and a CH–centroid angle of 139.0° (Figure 6a). The ketonic oxygen O1 forms a hydrogen bond with the neighboring molecule. The O1···H(-C8c) distance for the intermolecular hydrogen interaction is 2.464 Å (O1···C8c = 3.340 Å) and the corresponding O1···H-C8c angle is 156.9°. The hydrogen bond propagates, forming a chain (Figure 6b) (symmetry operation c = 2−x, −1/2+y, 3/2−z).

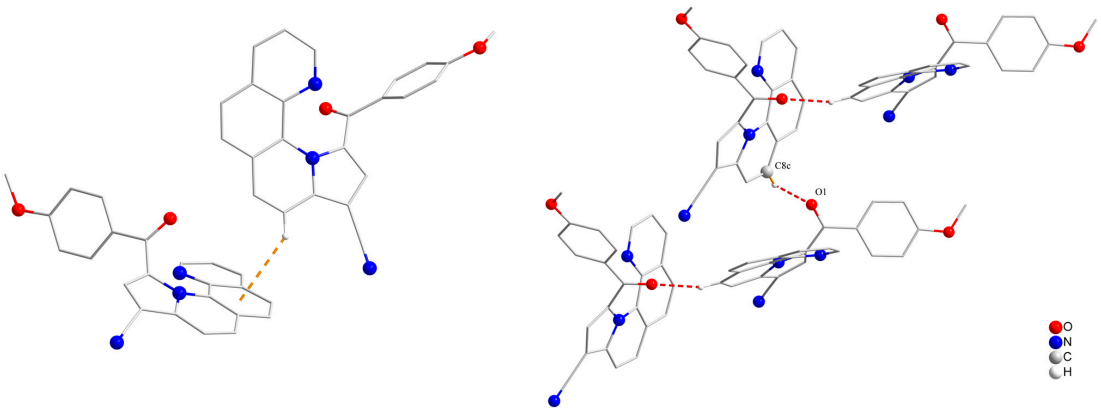

(**a**) (**b**)

Figure 6. Perspective view of **6c** showing (**a**) the CH–π interactions between two neighboring phenanthroline units, and (**b**) the hydrogen bond formed by the oxygen from the ketone unit (symmetry operation c = 2−x, −1/2+y, 3/2−z). Hydrogen atoms have been omitted, except those involved in hydrogen bonds and CH–π interactions.

Compound **6d** (Figure 3) crystalizes in a monoclinic crystal system, in the C2/*c* space group (Table 1). The dihedral angle ∠(C3-C4-C5),(C23-C18-C19), between the pyrrolic ring and the benzene ring, is 54.3°. The phenanthroline units are stacked, with π–π stacking centroid–centroid distances around 3.80 Å (Figure 7a). The ketonic oxygen O1 forms two hydrogen bonds with two neighboring molecules. The O1···H(-C23a) distance for the first intermolecular hydrogen interaction is 2.461 Å (O1···C23a = 3.140 Å) and the corresponding O1···H-C23a angle is 128.3°, while, for the second one, it is O1···H(-C7b) = 2.473 Å (O1···C7b = 3.187 Å) and the O1···H-C7b angle is 131.9° (Figure 7b) (symmetry operations a = 1−x, y, 1/2−z; b= 1−x, −y, 1−z).

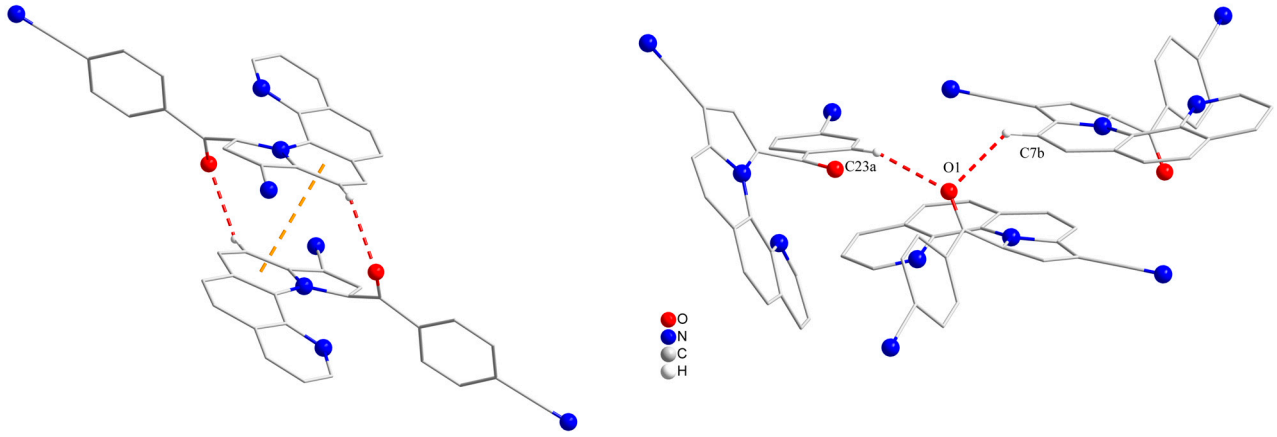

(**a**) (**b**)

Figure 7. Perspective view of **6d** showing (**a**) the π–π stacking interactions between two neighboring pyrrolo-phenanthroline units and (**b**) the hydrogen bonds formed by the oxygen from the ketone unit (symmetry operations a = 1−x, y, 1/2−z; b= 1−x, −y, 1−z). Hydrogen atoms have been omitted, except those involved in hydrogen bonds.

Among the compounds **6a**–**d**, it has been observed that the torsion angles from the phenanthroline unit ∠(N2-C17-C16-N3) vary between 6.7 and 7.8°, while the torsion angles between the pyrrolic ring and ketonic moiety, ∠(N2-C3-C1-O1), vary between 33.1 and 36.9°, respectively. The angle between the first pyrrolic ring (I) and the fourth aromatic ring (IV), ∠(C3-N2-C6),(N3-C16-C12), increases from 22.5 to 27.5°, with the volume of the substituents (Table 2). This dihedral angle values agree with those of similar compounds reported in the literature and are, in general, higher compared with the similar dihydro-pyrrolo-phenanthrolines (Table 3). Thus, helical conformations could be observed in the crystal structures, which generate P and M axial chirality. Both enantiomers are present in the crystal structure (Figure S1).

Table 2. Representative angles for compounds **6a**–**d**.

Compound	|∠(N2-C17-C16-N3)| */°	|∠(N2-C3-C1-O1)| */°	|∠(C3-N2-C6),(N3-C16-C12)| */°
6a	7.0	35.6	22.5
6d	7.2	35.0	23.2
6c	7.8	36.9	23.2
6b	6.7	33.1	27.5

* The numbers are presented as absolute values. The sign of the angles is either positive or negative for the two isomers (M and P).

Table 3. Representative torsion and dihedral angles from similar compounds reported in the literature.

	CSD Refcode *	DEWNID	GUMLEH	GUMLIL	ITOXAR	QAQCIV	POQHIO
Angles	|∠(N2-C17-C16-N3)|	5.4	1.7	3.4	2.0	5.5	6.2
	|∠(N2-C3-C1-O1)|	42.3	21.2	17.9	36.7	43.7	52.4
	|∠ (C3-N2-C6),(N3-C16-C12)|	22.8	9.1	2.5	21.9	18.8	21.3
Substituent	C4	-COO^iPr	$-PhCH_3$	-PhCl	-Ph	-COOEt	-COOEt
	C5	-COO^iPr	$-NO_2$	$-NO_2$	$-(CN)_2$	-H	-COOEt
	C21	-Ph	-H	-Cl	-H	-Ph	-H
	References	[34]	[12]	[12]	[7]	[33]	[40]

* The first four examples are similar dihydro-pyrrolo-phenanthrolines, while the other two are pyrrolo-phenanthrolines. For a general structure formula, see Figure 8.

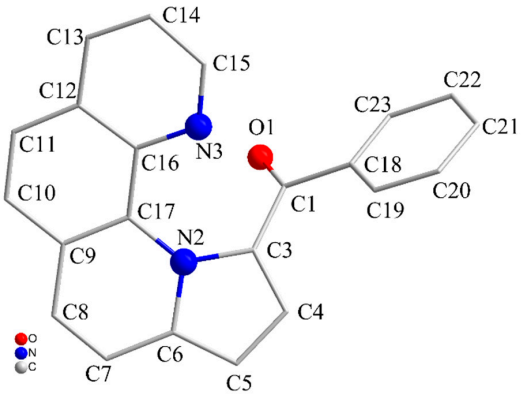

Figure 8. EThe common structure core and the numbering scheme shared by the compounds compared in Table 3. Hydrogen atoms are omitted. Substituents can be present on atoms C4, C5 and C21.

3.3. Photophysical Investigations (UV–Vis and Steady-State Photoluminescence Spectra)

The molar extinction coefficients as a function of the wavelength for compounds **6a–d** are shown in Figure 9.

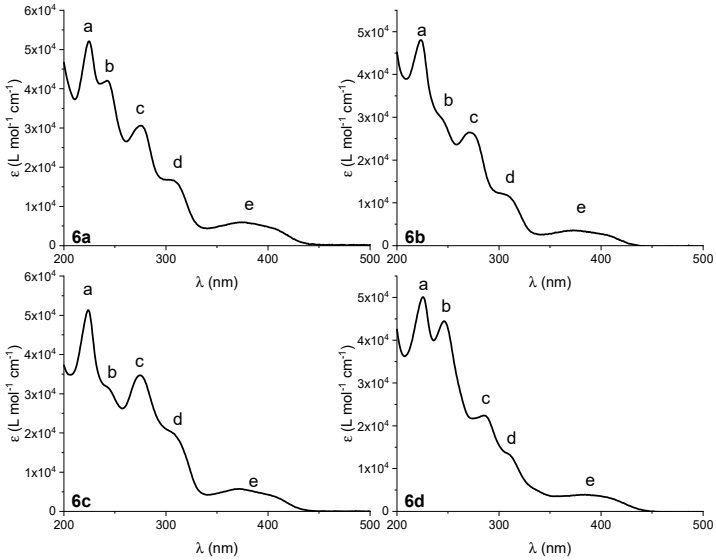

Figure 9. Molar extinction coefficient as a function of wavelength for the compounds **6a**−**d** in acetonitrile. The spectra were derived from the corrected UV–Vis spectra based on the Lambert–Beer law. The five peaks in each spectrum are labeled **a**−**e**. No absorption bands were seen at wavelengths higher than 500 nm. Each of the spectra shows five absorption bands in the measured region. The position of these bands is shown in Table 4.

Table 4. Electronic absorption band positions for compounds **6a–d** in acetonitrile. All values are given in nm.

Compound	6a	6b	6c	6d
Band **a**	225	223	224	225
Band **b**	242	244	242	246
Band **c**	276	271	275	285
Band **d**	304	306	304	310
Band **e**	372	372	372	384

There are no significant differences in the band positions for compounds **6a–c**, but bands **c** and **e** of compound **6d** show a 10 nm redshift. This could be attributed to the cyano substituent on the benzene ring, having an electron-withdrawing effect from both a resonance and an inductive perspective. Moreover, bands **a** and **b** are not redshifted because they correspond to the phenanthroline skeleton [39–42], which is at a considerable distance from the cyano substituent. The same bands were observed in other fused pyrrolo-1,10-phenanthroline type derivatives, where bands **c**, **d** and **e** were referred to as β, p and α, respectively [17].

The steady-state photoluminescence measurements revealed, in the case of all four compounds, two emission bands: one centered at around 350 nm and the other at around 500 nm (Figure 10).

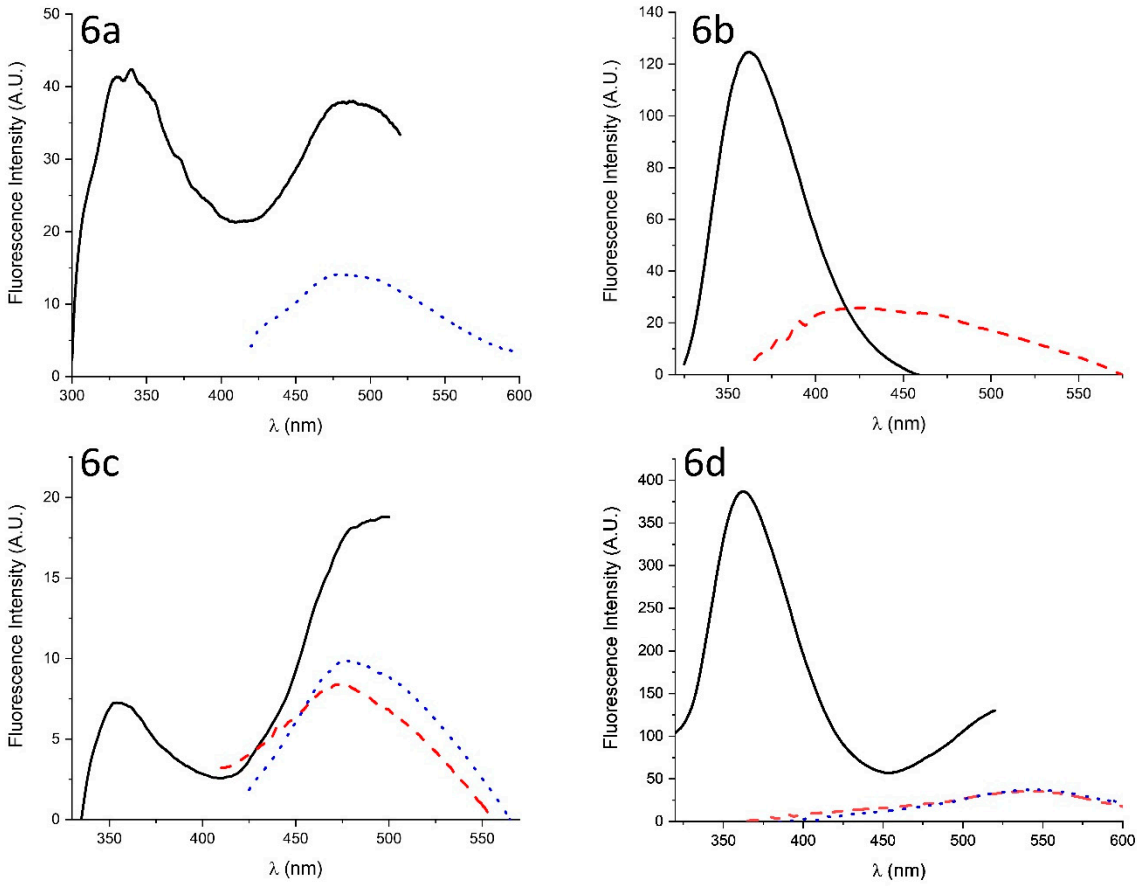

Figure 10. Emission spectra at λ_{ex} = 270 nm (black solid line), λ_{ex} = 350 nm (red dashed line) and λ_{ex} = 370 nm (blue dotted line) of compounds **6a–d** in acetonitrile. The excitation and emission slits for compound **6b** when excited at 270 nm were narrowed down to 3 nm each.

The exact maxima for each compound are presented in Table 4. In all cases, the overall emission is quite dim, for which reason the quantum yield was not measured. The most intense luminescence was observed in the case of compound **6b**, for which the excitation and emission slits needed to be narrowed down to 3 nm in order to avoid the saturation of the detector.

Table 5. Steady-state photoluminescence emission peak positions for compounds **6a**–**d** in acetonitrile. In each case, the excitation wavelength is given in brackets. All values are given in nm.

Compound	6a	6b	6c	6d
Band 1	339 (270)	361 (270)	356 (270)	363 (270)
Band 2	483 (370)	475 (315)	478 (370)	544 (370)

The emission spectra agree with previously published spectra of 1,10-phenanthroline derivatives, showing a primary band around 350 nm and a secondary, less intense and broader band at around 500 nm. It is unclear which photophysical processes cause the two different emissions, but we postulate that the first, more intense band corresponds to a singlet-state $S_1 \rightarrow S_0$ transition, either fluorescence or thermally activated delayed fluorescence (TADF), while the broader peak corresponds to a triplet-state phosphorescence. Previous studies described phosphorescence in 1,10-phenanthroline derivatives [43–45], while extended conjugated systems were reported to exhibit dual emission arising either from fluorescence and phosphorescence [46] or from phosphorescence and TADF [47]. Thus, an in-depth photophysical characterization is needed in order to fully understand the origin of the two emission bands.

Excitation spectra (Figure S2) were carried out to ensure that both emission peaks arose from the same species. The emission wavelength was, in each case, chosen on the blue side of the ~350 nm peak and on the red side of the ~500 nm peak, in order to minimize the contribution of the other peak in the spectrum (In Supplementary Materials).

4. Conclusions

Here, 9-cyano-pyrrolo[1,2-*a*][1,10]phenanthrolines were obtained by a one-pot procedure starting from 1,10-phenanthrolinium bromides, acrylonitrile and triethylamine, in the presence of an oxidant reagent. The synthesis implies the generation of an *N*-ylide from 1,10-phenanthrolinium, the [3+2] cycloaddition of the N-ylide to a dipolarophile, followed by the dehydrogenation of tetrahydro-pyrrolo[1,2-*a*][1,10]phenanthroline. The cycloaddition reaction's regioselectivity was deduced by H-NMR spectroscopy and further confirmed by X-ray diffraction. The investigated compounds present helical chirality with higher dihedral angles between cycles I and IV than in similar cycloadducts. Both enantiomers are present in the crystal structure. All compounds present similar photophysical properties, showing five bands in the absorption spectrum and two weak emission bands. Out of the four compounds, compound **6b** exhibits the strongest emission.

Supplementary Materials: The following supporting information can be downloaded at: https://www.mdpi.com/article/10.3390/cryst14010067/s1, Figure S1: Perspective views of the crystal structures of two neighboring enantiomers (M and P) of compounds **6a**–**d**. Hydrogen atoms have been omitted in the representations; Figure S2: Normalized absorption spectrum (black solid line) and normalized excitation spectrum for band 1 (dotted red line) and band 2 (solid red line) of compound **6a** ($\lambda_{em,1}$ = 330 nm, $\lambda_{em,2}$ = 500 nm), **6b** ($\lambda_{em,1}$ = 370 nm, $\lambda_{em,2}$ = 500 nm), **6c** ($\lambda_{em,1}$ = 370 nm, $\lambda_{em,2}$ = 500 nm), **6d** ($\lambda_{em,1}$ = 360 nm, $\lambda_{em,2}$ = 500 nm) in acetonitrile. The excitation and emission slits for compound **6b** when monitoring the emission at 370 nm were narrowed down to 3 nm each. $\lambda_{em,1}$ and $\lambda_{em,2}$ represent the wavelength at which the emission was monitored for band 1 and band 2, respectively; Figure S3: Thermal ellipsoid representation of the molecular structure of compounds **6a**–**d**.

Author Contributions: Conceptualization, F.D. and M.C.; methodology, F.D.; synthesis, M.C., L.A. and D.D.; analysis, M.R., S.S., C.D., V.A.N. and M.M.; writing—original draft preparation, M.C., M.R. and F.D.; writing—review and editing, M.C. and F.D. All authors have read and agreed to the published version of the manuscript.

Funding: This research received no external funding.

Data Availability Statement: Data are contained within the article and Supplementary Materials.

Conflicts of Interest: The authors declare no conflicts of interest.

References

1. Dumitrascu, F.; Mitan, C.I.; Draghici, C.; Caproiu, M.T.; Raileanu, D. Primary cycloadducts of 1,10-phenanthrolinium and phthalazinium phenacylides with DMAD. *Tetrahedron Lett.* **2001**, *42*, 8379–8382. [CrossRef]
2. Li, M.; Lv, X.L.; Wen, L.R.; Hu, Z.Q. Direct Solvent-Free Regioselective Construction of Pyrrolo[1,2-a][1,10]phenanthrolines Based on Isocyanide-Based Multicomponent Reactions. *Org. Lett.* **2013**, *15*, 1262–1265. [CrossRef] [PubMed]
3. Marandi, G.; Hazeri, N.; Maghsoodlou, M.T.; Habibi-Khorassani, S.M.; Torbati, N.A.; Rostami-Charati, F.; Skelton, B.W.; Makha, M. Synthesis of Cyano-pyrrolo[1,2-a][1,10]phenanthroline Derivatives Using a Multicomponent Condensation. *J. Heterocycl. Chem.* **2013**, *50*, 568–572. [CrossRef]
4. Dumitrascu, F.; Caira, M.R.; Draghici, C.; Caproiu, M.T.; Badoiu, A. 1,3-Dipolar Cycloaddition Reactions of 1-(4-Phenylphenacyl)-1,10-phenanthrolinium N-Ylide with Activated Alkynes and Alkenes. *Molecules* **2005**, *10*, 321–326. [CrossRef] [PubMed]
5. Dumitrascu, F.; Caira, M.R.; Draghici, C.; Caproiu, M.T.; Barbu, L.; Dumitrescu, D.G. Enhancing the helical distortion in pyrrolo[1,2-a][1,10]phenanthrolines. *Arkivoc* **2010**, *(ix)*, 97–107. [CrossRef]
6. Heydari, R.; Tahamipour, B. Highly regioselective synthesis of dicyano-8a,10,11-trihydropyrrolo [1,2-*a*][1,10]phenanthrolines via a domino-Knoevenagel-cyclization. *Chin. Chem. Lett.* **2011**, *22*, 1281–1284. [CrossRef]
7. Tahamipour, B.; Heydari, R.; Torbati, N.A.; Ziyaadini, M.; Graiff, C. Diastereoselective synthesis and X-ray structure of new stable dicyano(8aRS,10SR,11SR)-9,9-dicyano-10-aryl-11-benzoyl-8a,9,10,11-tetrahydropyrrolo[1,2-a][1,10]phenanthrolines. *J. Chem. Res.* **2011**, *35*, 329–332. [CrossRef]
8. Heydari, R.; Tahamipour, B.; Torbati, N.A.; Graiff, C.; Ziyaadini, M. One-Pot Synthesis and X-Ray Structure of New, Stable Tetrahydropyrrolo[1,2-a][1,10]phenanthrolines with Four Diastereoisomeric Centers. *Synth. Commun.* **2013**, *43*, 2031–2041. [CrossRef]
9. Dhinamkaran, I.; Padmini, V.; Ganesan, K.; Selvarasu, K. A-One Pot Four Component and Microwave-Assisted Synthesis of Pyrrolo [1, 10]phenanthrolines. *ChemistrySelect* **2017**, *2*, 6154–6158. [CrossRef]
10. Dumitrascu, F.; Caira, M.R.; Draghici, C.; Caproiu, M.T.; Barbu, L.; Miu, B. New 1,10-phenanthroline derivatives with potential antitumoral activity. *Rev. Roum. Chim.* **2008**, *53*, 183–187.
11. Dürüst, Y.; Sağırlı, A.; Fronczek, F.R. Regioselective 1,3-dipolar cycloaddition of phenanthrolinium N-ylides to substituted arylidene oxazolones. *Mol. Divers.* **2011**, *15*, 799–808. [CrossRef] [PubMed]
12. Liu, Z.M.; Fang, J.; Yan, C.G. Diastereoselective Synthesis of 1,10-Dihydropyrrolo[1,2-a][1,10]phenanthroline Derivatives via 1,3-Dipolar Cycloaddition Reaction. *Chem. Res. Chin. Univ.* **2013**, *29*, 1089–1093. [CrossRef]
13. Danac, R.; Rotaru, A.; Drochioiu, G.; Druta, I. Synthesis of Novel Phenanthroline Derivatives by 3+2 Dipolar Cycloadition Reaction. *J. Heterocycl. Chem.* **2003**, *40*, 283–287. [CrossRef]
14. Danac, R.; Constantinescu, M.; Rotaru, A.; Vlahovici, A.; Cretescu, I.; Druta, I. Study ofDipolar 3+2 Cycloaddition Reaction of 1,10-Phenanthrolinium Ylides to Activated Alkenes. *Rev. Chim.* **2005**, *56*, 85–88.
15. Dumitrascu, F.; Draghici, C.; Caira, M.R.; Badoiu, A.; Barbu, L.; Cristea, M. 1,3-Dipolar cycloaddition reactions of 1-(3-nitrophenacyl)-1,10-phenanthrolinium N-ylide with activated alkynes. *Arkivoc* **2005**, *x*, 165–173. [CrossRef]
16. Dumitrascu, F.; Caira, M.R.; Draghici, C.; Caproiu, M.T.; Barbu, L. Isolation and X-Ray Structure of an Intermediate in 1,3-Dipolar Cycloaddition of 1,10-Phenanthrolinium N-Ylides with Alkynes: 1,2-Dihydropyrrolo-[1,2-a][1,10]phenanthroline. *Rev. Chim.* **2009**, *60*, 851–854.
17. Al-Matarneh, C.M.; Rosca, I.; Shova, S.; Danac, R. Synthesis and properties of new fused pyrrolo-1,10-phenanthroline type derivatives. *J. Serb. Chem. Soc.* **2021**, *86*, 901–915. [CrossRef]
18. Stępień, B.T.; Krygowski, T.M.; Cyrański, M.K.; Młochowski, J.; Orioli, P.; Abbate, F. How far is the π-electron delocalization of the phenanthrene moiety modified in the aza-analogues and their N-oxides? *Arkivoc* **2004**, *iii*, 185–201. [CrossRef]
19. Bazzicalupi, C.; Bencini, A.; Bianchi, A.; Borsari, L.; Danesi, A.; Giorgi, C.; Lodeiro, C.; Mariani, P.; Pina, F.; Santarelli, S.; et al. Basicity and coordination properties of a new phenanthroline-based bis-macrocyclic receptor. *Dalton Trans.* **2006**, *33*, 4000–4010. [CrossRef]
20. Schoffers, E. Reinventing Phenanthroline Ligands—Chiral Derivatives for Asymmetric Catalysis? *Eur. J. Org. Chem.* **2003**, *7*, 1145–1152. [CrossRef]
21. Danac, R.; Al Matarneh, C.M.; Shova, S.; Daniloaia, T.; Balan, M.; Mangalagiu, I.I. New indolizines with phenanthroline skeleton: Synthesis, structure, antimycobacterial and anticancer evaluation. *Bioorg. Med. Chem.* **2015**, *23*, 2318–2327. [CrossRef] [PubMed]

22. Al Matarneh, C.M.; Shova, S.; Mangalagiu, I.I.; Danac, R. Synthesis, structure, antimycobacterial and anticancer evaluation of new pyrrolo-phenanthroline derivatives. *J. Enz. Inhib. Med. Chem.* **2016**, *31*, 470–480. [CrossRef] [PubMed]
23. Roy, S.; Hagan, K.D.; Maheswari, P.U.; Lutz, M.; Spek, A.L.; Reedijk, J.; van Wezel, G.P. Phenanthroline derivatives with improved selectivity as DNA-targeting anticancer or antimicrobial drugs. *ChemMedChem* **2008**, *3*, 1427–1434. [CrossRef]
24. Sall, C.; Yapi, A.-D.; Desbois, N.; Chevalley, S.; Chezal, J.-M.; Tan, K.; Teulade, J.-C.; Valentin, A.; Blache, Y. Design, synthesis, and biological activities of conformationally restricted analogs of primaquine with a 1,10-phenanthroline framework. *Bioorg. Med. Chem. Lett.* **2008**, *18*, 4666–4669. [CrossRef] [PubMed]
25. Nielsen, M.C.; Larsen, A.F.; Abdikadir, F.H.; Ulven, T. Phenanthroline- 2,9-bistriazoles as selective G-quadruplex ligands. *Eur. J. Med. Chem.* **2014**, *72*, 119–126. [CrossRef] [PubMed]
26. Wesselinova, D.; Neykov, M.; Kaloyanov, N.; Toshkova, R.; Dimitrov, G. Antitumour activity of novel 1,10-phenanthroline and 5-amino-1,10-phenanthroline derivatives. *Eur. J. Med. Chem.* **2009**, *44*, 2720–2723. [CrossRef] [PubMed]
27. Leontie, L.; Druta, I.; Danac, R.; Rusu, G.I. On the electronic transport properties of pyrrolo[1,2-*a*][1,10]phenanthroline derivatives in thin films. *Synth. Met.* **2005**, *155*, 138–145. [CrossRef]
28. Leontie, L.; Druta, I.; Danac, R.; Prelipceanu, M.; Rusu, G.I. Electrical properties of some new high resistivity organic semiconductors in thin films. *Prog. Org. Coat.* **2005**, *54*, 175–181. [CrossRef]
29. Al Matarneh, C.M.; Danac, R.; Leontie, L.; Tudorache, F.; Petrila, I.; Iacomi, F.; Carlescu, A.; Nedelcu, G.; Mangalagiu, I. Synthesis and electron transport properties of some new 4,7-phenanthroline derivatives in thin films. *Environ. Eng. Manag. J.* **2015**, *14*, 421–431.
30. Prelipceanu, M.; Prelipceanu, O.S.; Leontie, L.; Danac, R. Photoelectron spectroscopy investigations of pyrrolo[1,2-*a*][1,10]phenanthroline derivatives. *Phys. Lett. A* **2007**, *368*, 331–335. [CrossRef]
31. Accorsi, G.; Listorti, A.; Yoosaf, K.; Armaroli, N. 1,10-Phenanthrolines: Versatile building blocks for luminescent molecules, materials and metal complexes. *Chem. Soc. Rev.* **2009**, *38*, 1690–1700. [CrossRef]
32. Prelipceanu, M.; Prelipceanu, O.S. Study of thermal conversion and patterning of a new soluble poly (*p*-phenylenevinylene) (PPV) precursor. *Mater. Sci. Semicond. Process* **2007**, *10*, 77–89. [CrossRef]
33. Dumitrascu, F.; Caira, M.R.; Draghici, C.; Caproiu, M.T.; Barbu, L.; Badoiu, A. Helical chirality of pyrrolo[1,2-*a*][1,10]phenanthroline derivatives. *J. Chem. Crystallogr.* **2005**, *35*, 361–365. [CrossRef]
34. Dumitrascu, F.; Caira, M.R.; Draghici, C.; Caproiu, M.T. Crystal Structure of a New Pyrrolo[1,2-*a*][1,10]phenanthroline Derivative. *Anal. Sci. X-ray Struct. Anal. Online* **2007**, *23*, X13–X14. [CrossRef]
35. Dumitrascu, F.; Dumitrescu, D.G.; Aron, I. Azahelicenes and other similar tri and tetracyclic helical molecules. *Arkivoc* **2010**, *i*, 1–32. [CrossRef]
36. Dolomanov, O.V.; Bourhis, L.J.; Gildea, R.J.; Howard, J.A.K.; Puschmann, H. OLEX2: A complete structure solution, refinement and analysis program. *J. Appl. Crystallogr.* **2009**, *42*, 339–341. [CrossRef]
37. Sheldrick, G.M. SHELXT—Integrated space-group and crystal-structure determination. *Acta Crystallogr. Sect. A Found. Adv. A* **2015**, *71*, 3–8. [CrossRef]
38. Sheldrick, G.M. Crystal structure refinement with SHELXL. *Acta Crystallogr. C Struct. Chem.* **2015**, *71*, 3–8. [CrossRef]
39. Hu, Y.; Hu, H. A Versatile Oxidizing Agent: Tetrakis-pyridino-cobalt(II) Dichromate $Py_4Co(HCrO_4)_2$ (TPCD). Oxidations of Alcohols, Halides and Amines to Their Corresponding Carbonyl Compounds. *Synth. Commun.* **1992**, *22*, 1491–1496. [CrossRef]
40. Paira, R.; Anwar, T.; Banerjee, M.; Bharitkar, Y.P.; Mondal, S.; Kundu, S.; Hazra, A.; Maulik, P.R.; Mondal, N.B. Copper–Phenanthroline Catalysts for Regioselective Synthesis of Pyrrolo[3′,4′:3,4]Pyrrolo[1,2-a]Furoquinolines/Phenanthrolines and of Pyrrolo[1,2-a]Phenanthrolines under Mild Conditions. *Beilstein J. Org. Chem.* **2014**, *10*, 692–700. [CrossRef]
41. Linnell, R.H.; Kaczmarczyk, A. Ultraviolet spectra of [Ill] compounds[1]. *J. Phys. Chem.* **1961**, *65*, 1196–1200. [CrossRef]
42. Tammiku, J.; Burk, P.; Tuulmets, A. UV-vis spectrum of the 1,10-phenanthroline-ethylmagnesium bromide complex. An experimental and computational study. *Main Gr. Met. Chem.* **2000**, *23*, 301–305. [CrossRef]
43. Brinen, J.S.; Rosebrook, D.D.; Hirt, R.C. Phosphorescence of *o*-phenanthroline[1]. *J. Phys. Chem.* **1963**, *67*, 2651–2655. [CrossRef]
44. Sun, W.; Shi, B.; Xia, Z.; Lü, C. Visible-light-excited long-lived organic room-temperature phosphorescence of phenanthroline derivatives in PVA matrix by H-bonding interaction for security applications. *Mater. Today Chem.* **2023**, *27*, 101297. [CrossRef]
45. Sun, W.; Hu, W.; Shi, B.; Lü, C. 1,10-Phenanthroline-5-amine derived N-doped carbon dots for long-lived visible-light-activated room temperature phosphorescence in the matrix and information encryption application. *J. Lumin.* **2023**, *263*, 120078. [CrossRef]
46. Salas Redondo, C.; Kleine, P.; Roszeitis, K.; Achenbach, T.; Kroll, M.; Thomschke, M.; Reineke, S. Interplay of Fluorescence and Phosphorescence in Organic Bituminescent Emitters. *J. Phys. Chem. C.* **2017**, *121*, 14946–14953. [CrossRef] [PubMed]
47. Schwendt, G.; Borisov, S.M. Achieving simultaneous sensing of oxygen and temperature with metalloporphyrins featuring efficient thermally activated delayed fluorescence and phosphorescence. *Sens. Actuators B Chem.* **2023**, *393*, 134236. [CrossRef]